



UNIVERSITY OF LEEDS

This is a repository copy of *Investigation of Molten Salt Phase Formation during Alkali Roasting of Titaniferous Minerals with Sodium and Potassium Hydroxide*.

White Rose Research Online URL for this paper:
<http://eprints.whiterose.ac.uk/110008/>

Version: Accepted Version

Article:

Parirenyatwa, S, Escudero Castejon, L orcid.org/0000-0003-1525-0435, Sanchez Segado, S orcid.org/0000-0002-3511-0723 et al. (2 more authors) (2016) Investigation of Molten Salt Phase Formation during Alkali Roasting of Titaniferous Minerals with Sodium and Potassium Hydroxide. *Journal for Manufacturing Science and Production*, 16 (4). ISSN 0793-6648

<https://doi.org/10.1515/jmsp-2016-0025>

© 2017, Walter de Gruyter GmbH. This is an author produced version of a paper published in *Journal for Manufacturing Science and Production*. Uploaded in accordance with the publisher's self-archiving policy.

Reuse

Unless indicated otherwise, fulltext items are protected by copyright with all rights reserved. The copyright exception in section 29 of the Copyright, Designs and Patents Act 1988 allows the making of a single copy solely for the purpose of non-commercial research or private study within the limits of fair dealing. The publisher or other rights-holder may allow further reproduction and re-use of this version - refer to the White Rose Research Online record for this item. Where records identify the publisher as the copyright holder, users can verify any specific terms of use on the publisher's website.

Takedown

If you consider content in White Rose Research Online to be in breach of UK law, please notify us by emailing eprints@whiterose.ac.uk including the URL of the record and the reason for the withdrawal request.



eprints@whiterose.ac.uk
<https://eprints.whiterose.ac.uk/>

Investigation of Molten Salt Phase Formation during Alkali Roasting of Titaniferous Minerals with Sodium and Potassium Hydroxide

S.Parirenyatwa, L.Escudero-Castejon, S.Sanchez-Segado, Y.Hara, A.Jha

Institute for Materials Research, School of Chemical and Process Engineering
Faculty of Engineering, University of Leeds
Leeds LS2 9JT

Abstract

The benefit of alkali roasting over existing processes is that it minimises waste and energy consumption compared with the current methods for the beneficiation of titaniferous minerals. Previous studies on the liquid phase formation during alkali roasting of titaniferous minerals were based on the use of Na_2CO_3 , whereas this study focuses on the oxidative roasting of ilmenite with either NaOH or KOH , using different alkali to mineral ratios, in air at 1000°C . This work attempts to characterise the alkali-rich liquid phase formed during roasting and determine its impact on the physical chemistry of roasting. Phase equilibria of the Na/K-Fe-Ti-O systems were calculated and compared with experimental results. Samples roasted with NaOH demonstrated segregation of Ti and Fe oxides, but only Ti-K-Fe-O ternary compound were present in products treated with KOH . The presence of the liquid phase at the reaction interface adversely affects the oxygen diffusion during roasting, which has influence on the products formed.

Introduction

The primary natural feedstocks used for the production of titanium chemicals are: ilmenite (FeTiO_3); rutile (TiO_2) and leucocoxene ($\text{Fe}_2\text{O}_3\cdot\text{TiO}_2$). These titanium bearing minerals are largely used to produce pigment grade TiO_2 , with a smaller amount (approx. 10%) dedicated to the production of Ti metal [1]. Pigment grade TiO_2 is mainly used for paper, plastics, paints and coatings industries. The two primary routes for TiO_2 pigment production are the sulphate and chloride processes, with the latter being the most widely used because of its economic and environmental advantages [2]. However, the scarcity of high-grade titaniferous minerals required for the chloride process, has led to an increase in the use of synthetic rutile and TiO_2 -rich slag as feedstock and to the investigation of alternative methods for the beneficiation of low grade- minerals [3].

The application of alkali roasting in oxidative conditions dates back to the days of Le Chatelier in the 19th century, where he initially used this method for the treatment of bauxite and chromite ores [4]. More recently, the alkali roasting technique has been employed for the physico-chemical separation of reactive metal oxides from complex minerals [5].

Foley and Mackinnon [6], reported the formation of Na/K-Fe-Ti-O and Fe_2O_3 oxides after the alkali roasting of ilmenite with potassium and sodium carbonates at 860°C in air atmosphere. After roasting the products were leached in 20% HCl solution pointing out that iron removal was higher for Na_2CO_3 roasted samples. Lahiri and Jha [7] investigated the kinetics and reaction mechanism of ilmenite roasting with Na_2CO_3 , in the temperature range 600°C - 900°C temperature range. They reported on the formation of the sodium iron titanate phase as an intermediate that rearranged to produce sodium ferrite and release TiO_2 from the lattice. A new technique to selectively separate rare-earth oxides (REO) from bomar ilmenite was demonstrated by Lahiri and Jha [8]. They roasted bomar ilmenite with KOH , which liberated

the rare-earth oxides from the mineral matrix and then proceeded to water leach the residue in order to concentrate the REO in a colloidal layer. The formation of a Na-Ti-Fe-O ternary phase at temperatures above 550°C was reported by Manhique et al. [9] when NaOH was used as a roasting agent but below this temperature sodium titanate and sodium ferrite were the dominant phases. A study on the effects of roasting bomar ilmenite with potassium, sodium and lithium carbonates and hydroxides was reported by Sanchez Segado et al [10]. The roasted products were water leached to separate the REO as a colloidal suspension and leave behind alkali titanate rich residues, which were subsequently leached in oxalic and ascorbic acid solutions in order to precipitate high-purity synthetic rutile. Parirenyatwa et al. [11] performed a comparative study of the oxidative roasting of ilmenite with either KOH or NaOH in the temperature range of 700°C – 1000°C, and identified the presence of alkali iron titanates. Liu et al [12] carried out NaOH molten salt roasting of titanium-vanadium slag at 550°C, where response surface methodology was used to optimize roasting conditions. A residue containing 98 wt. % TiO₂ was obtained after leaching with sulphuric acid.

A key step towards the commercialisation of the alkali roasting process is understanding the role of the liquid phase during the roasting reaction. This liquid phase is not only found to limit oxygen diffusion but also creates operational problems like ring formation in rotary kilns. Previous studies by Tathavadkar and Jha on liquid phase formation during alkali roasting of titaniferous minerals were based on the using Na₂CO₃ to roast ilmenite and anatase, followed by acid leaching (HCl) so as to beneficiate the titaniferous minerals [13]. It was noticed that excess soda ash increases the volume of the liquid phase, improving the purity of synthetic rutile obtained after water and acid leaching. Excess addition of alkali led to the formation of a complex salt phase that enhanced the thermodynamic stability of sodium ferrite and promoted the separation of iron oxide from the titanium-rich phase.

This study focuses on the oxidative roasting of titaniferous minerals with either NaOH or KOH at different alkali ratios in order to address the influence of the liquid phase on the separation of alkali titanates and alkali ferrites.

2. Experimental

2.1 Materials

Ilmenite mineral with a particle size of 106µm was used for this investigation. Potassium hydroxide (KOH) or sodium hydroxide (NaOH) of analytical reagent grade were used for the oxidative roasting experiments.

Crystal structure

Ilmenite has a hexagonal structure with, titanium and iron cations forming alternating bilayers perpendicular to the c axis, as it can be seen in Figure 1 [14]. The Ti and Fe ions are both octahedrally coordinated to the O ions.

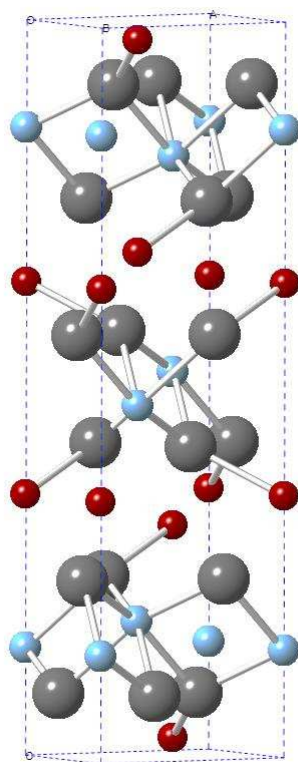


Figure 1. Crystal structure of ilmenite mineral (O = grey, Ti = blue, Fe = red)

The ilmenite mineral was characterized using X-ray powder diffraction (XRPD), X-ray fluorescence (XRF) and scanning electron microscopy – energy dispersive X-ray spectroscopy (SEM-EDX). The chemical composition of the mineral is presented in table I. The size difference between Fe^{2+} (0.92\AA) and Mn^{2+} (0.97\AA) is less than 15%, therefore atomic substitutions between the two ions are possible allowing the manganese to exist as a substitutional impurity[15].

Table I. Chemical composition of ilmenite mineral used for roasting experiments, as analysed by X-ray fluorescence.

Wt. %	TiO ₂	Fe ₂ O ₃	MnO	V ₂ O ₅	Al ₂ O ₃	SiO ₂
	51.2	44.5	1.48	0.34	0.91	0.59

The XRPD pattern of the ilmenite mineral is presented in figure 2. The main phases identified in the mineral are ilmenite (FeTiO_3), pseudorutile ($\text{Fe}_2\text{Ti}_3\text{O}_9$) and titanium aluminium oxide, with ilmenite as the major phase present.

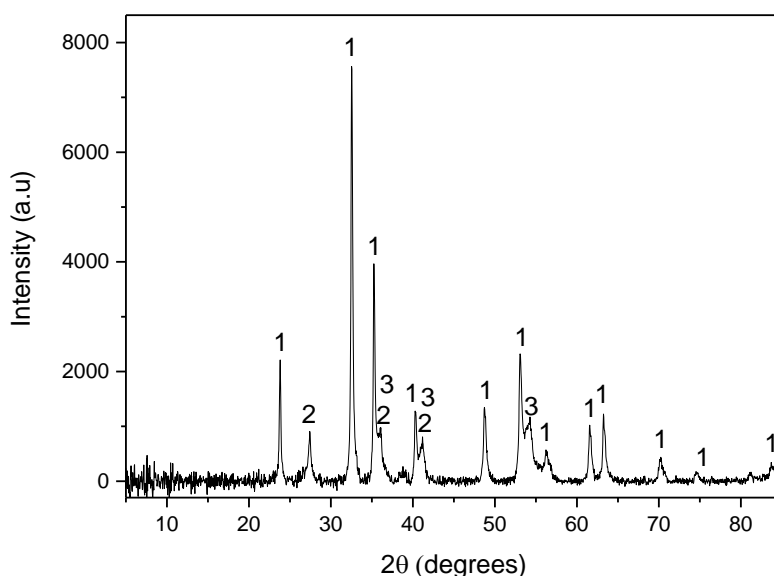


Figure 1. X-ray powder diffraction pattern of ilmenite ore. 1 = FeTiO_3 (01-075-1209), 2 = $\text{Fe}_2\text{Ti}_3\text{O}_9$ (00-019-0635), 3 = $\text{Ti}_{0.984}\text{Al}_{0.016}\text{O}_{1.992}$ (04-008-2608)

Backscattered SEM images of the as-received ilmenite sample are presented in figures 3a and b. SEM elemental mapping and EDX indicated the presence of manganese and aluminum as solid solutions with the ilmenite phase. Examination of the particle in figure 3b shows that there are two distinct phases. The dark-grey phase (Area A in Table II) is a titanium-rich area that corresponds to the pseudorutile phase observed in the XRPD pattern in figure 2. Teufer and Temple identified that this phase is formed due to chemical modifications of ilmenite during natural weathering [16]. The ferrous iron is oxidised to ferric iron before one-third of the ferric iron is leached out [17], as can be observed in the elemental mappings shown in figure 3b. Weathering also led to the leaching out of manganese, as it can be seen in the manganese column of Table II for Area A. Analysis of the light grey phase (Area B in Table II) indicates that the composition of this phase is in line with that of ilmenite. A low magnification image of the ilmenite mineral (figure 3a), demonstrates that ilmenite is the dominant phase with the presence of some weathered particles. The SEM analysis agrees with the results observed in the XRPD pattern (figure 2), where ilmenite is the main phase with pseudorutile and titanium aluminium oxide as minor phases

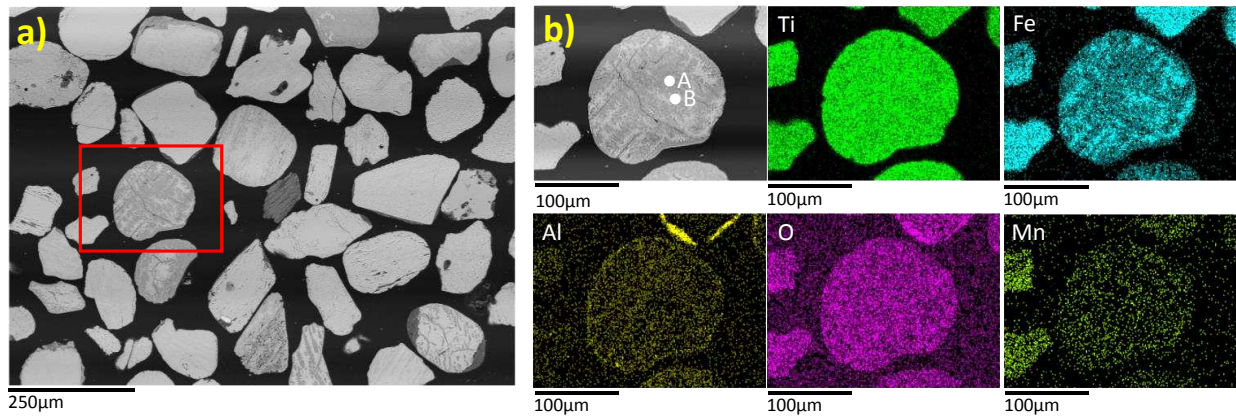


Figure 3. Backscattered scanning electron microscopy images of the as-received ilmenite mineral a) low-magnification image and b) elemental mapping.

Table II. Elemental composition of areas A and B in Figure 3b analysed by SEM-EDX.

%Wt	Ti	Fe	O	Mn	Al
A	49.5	13.3	35.7	-	1.2
B	33.6	36.8	27.9	1.0	0.7

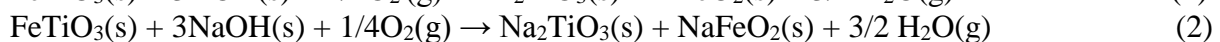
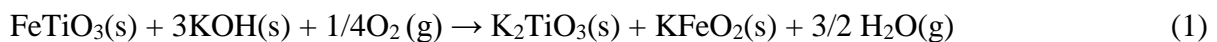
2.2 Experimental procedure

Ilmenite mineral samples were mixed with either KOH or NaOH, based on the amount needed to produce alkali titanate and alkali ferrite. The $\text{FeTiO}_3\text{:MOH}$ ratios used were 1:3, 1:4.5 and 1:6, which represents the stoichiometric, 1.5 and 2 times stoichiometric amounts, respectively. The reaction mixture was ground and thoroughly mixed before being placed in an alumina crucible. The alumina crucible was placed in a resistance furnace at 1000°C for 2 hours in air. After roasting, the samples were leached in hot water (90°C) for 1 hour with continuous stirring throughout the leaching process. Following leaching, the samples were filtered using Whatman filter paper and then dried in an oven at 90°C . The dried residues were analysed using SEM-EDX. The dried residues were heated at 800°C in order to increase their crystallinity prior to XRPD analysis. A Philips X'Pert X-ray diffractometer was used for XRPD analysis of the powder samples over an angle 2θ from 5° to 85° , using $\text{Cu-K}\alpha$ radiation. The X'Pert HighScore Plus database software was used for phase-identification of the XRPD patterns.

3. Results and Discussion

3.1 Thermodynamic evaluation

The roasting of ilmenite with alkali in air atmosphere results in the oxidation of iron from the 2+ state to the 3+ state, with the aim of separating iron oxide from titanium dioxide by forming alkali ferrites and alkali titanates, respectively. The reactions with potassium hydroxide and sodium hydroxide are expected to proceed according to equations (1) and (2), respectively.



Free energy calculations performed using HSC 5.1 shown that reaction 1 is more thermodynamically favourable than reaction 2 at 1000°C, with free energy values of -911 kJ and -240kJ and, respectively [18].

Phase diagrams

Figures 4a and 4b are the ternary phase diagrams for K₂O-Fe₂O₃-TiO₂ and Na₂O-Fe₂O₃-TiO₂, respectively, calculated using the FACTSage software [19]. It can be observed from figure 4a that as the alkali content increases the liquid phase is present in the form of K₄TiO₄(l) and K₂O(l) in the K-Ti-Fe-O system. However, the calculations indicate that no liquid phases are formed in the Na-Fe-Ti-O system (figure 4b). The alkali ferrite phases are presented in both figures 4a and 4b. No ternary phases are predicted possibly due to the lack of thermodynamic data in the FACTSage database. However, thermodynamic data for KFeO₂ from HSC 5.1 [18] was inputted into the FACTSage database.

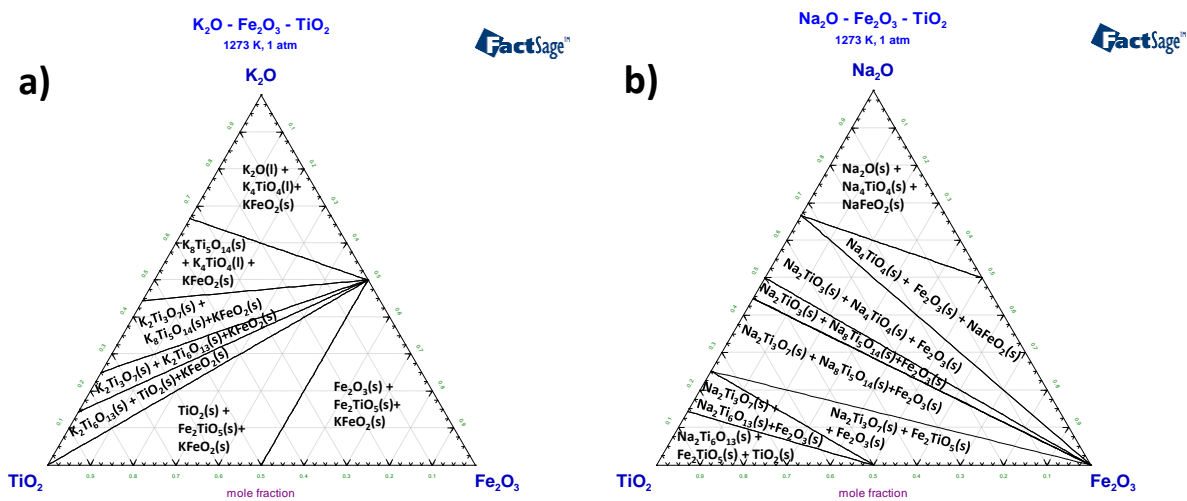


Figure 4. The ternary phase diagrams of a) K₂O-Fe₂O₃-TiO₂ b) Na₂O-Fe₂O₃-TiO₂, computed at 1000 °C using FACTSage software [19].

Phase equilibria calculations

In order to predict the phases formed during the roasting with different alkali ratios, phase equilibria calculations were performed utilising the Gibbs energy minimisation technique with the FACTSage software [19]. The data used in the calculations correspond to the experimental quantities employed, and the results are presented in Table III. When the stoichiometric amount of KOH is used KFeO₂, K₄TiO₄(l) and K₈Ti₅O₁₄ are the phases that co-exist. Excess KOH addition results in a decrease in the amount K₈Ti₅O₁₄ phase present and promotes the formation of a liquid phase mainly composed of K₄TiO₄(l). The liquid phase inhibits oxygen diffusion and can thus limit the oxidation of FeO to Fe₂O₃, which is important because it creates vacancies in the ilmenite lattice that enhance the mineral reactivity [13].

The phase equilibria calculations performed for the ilmenite roasting with NaOH predicted the formation Na₄TiO₄, Na₂TiO₃ and Fe₂O₃ for the stoichiometric amount of alkali salt. For higher ratios the amount of NaFeO₂ is expected to increase meanwhile the Na₂TiO₃ phase disappears. At twice the stoichiometric amount of NaOH the hematite phase is completely replaced with NaFeO₂. This is in agreement with the previous study of Tathavadkar and Jha which found that higher alkali amounts improved the separation of iron oxide [13].

Table III. Composition of roasting charge and equilibrium phase composition calculated using FACTSage software for roasting of ilmenite with either KOH or NaOH, with different molar ratios[19].

	KOH				NaOH		
Stoichiometry	1x	1.5x	2x	Stoichiometry	1x	1.5x	2x
Species	Moles			Species	Moles		
FeTiO ₃	0.033	0.033	0.033	FeTiO ₃	0.033	0.033	0.033
KOH	0.099	0.148	0.198	NaOH	0.099	0.148	0.198
O ₂ (g)	0.008	0.008	0.008	O ₂ (gas)	0.008	0.008	0.008
Equilibrium phase composition (moles)							
Species				Species			
KFeO ₂ (s)	0.033	0.033	0.033	Na ₄ TiO ₄ (s)	0.016	0.033	0.033
K ₄ TiO ₄ (l)	0.005	0.026	0.033	Fe ₂ O ₃ (s)	0.016	0.008	0.0
K ₈ Ti ₅ O ₁₄ (s)	0.005	0.001	0.0	Na ₂ TiO ₃ (s)	0.016	0.0	0.0
KOH(l)	0.0	0.0	0.027	NaFeO ₂ (s)	0.0	0.016	0.033
				NaOH(l)	0.0	0.0	0.032
H ₂ O(g)	0.998	0.998	0.939	H ₂ O(gas)	1.000	1.000	0.994

Water leaching

The water leaching of the roasted products is expected to proceed via reactions (3), (4) and (5), where the water-soluble alkali ferrites are hydrolysed allowing for the recovery of the alkali hydroxides and the formation of Fe₂O₃, which precipitates as Fe(OH)₃. This causes an increase of the solution pH, which was observed during the leaching process.



The E_h-pH diagrams for the Fe-K-Ti-H₂O and Fe-Na-Ti-H₂O systems at 90°C are presented in figures 5a and 5b, respectively. Figure 5a shows that the stable compounds present during water leaching, are water-soluble KOH and insoluble Fe₂O₃ and TiO₂. However, potassium titanates were expected to be present in the solid residue according to the results reported by other authors[20]. The absence of potassium titanates in the stability region of water, in figure 5a, may be due to limitations in thermochemical data available in the FACTSage software. Previous studies on the hydrothermal leaching of ilmenite with KOH, put into manifest the presence of various potassium titanates in the leaching residue. Acid leaching of these residues was carried out to produce high-grade TiO₂ [21-23]. Figure 5b, the Fe-Na-Ti-H₂O system, shows that in the pH range 10.5 to 12.9 the stable phases are Fe₂O₃, various sodium titanates (Na₂Ti₆O₁₃, Na₂Ti₃O₇ and Na₂TiO₃) and NaOH. It is also depicted that for pH values above 12.9 the stable phases are Fe₂O₃, Na₂TiO₃ and Na₄TiO₄.

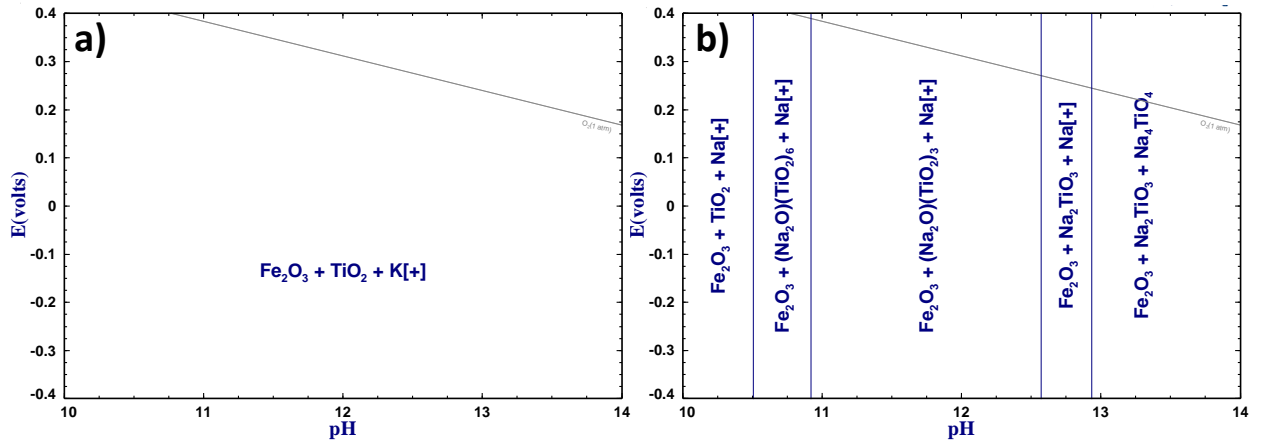


Figure 5. E_h -pH diagrams for the a) Fe-K-Ti-H₂O and b) Fe-Na-Ti-H₂O system at 383K computed using FACTSage 6.4 software[19].

3.2 Experimental results

Effect of roasting on phases formed

The XRPD patterns for the water leached residues after KOH roasting of the ilmenite with different stoichiometric ratios are presented in figures 6a-c. The ternary phases formed have a $K_xFe_xTi_{1-x}O_2$ composition, which has a potassium deficient α -KFeO₂ structure [6]. Figure 6a shows that the stoichiometric amount of alkali led to the formation of two different potassium iron titanate phases, with $K_{0.4}Ti_{0.6}Fe_{0.4}O_2$ as the dominant phase and $K_{0.85}Fe_{0.85}Ti_{0.15}O_2$ as a minor phase. Figures 6b and 6c show that as the alkali ratio increases, the intensity of the $K_{0.85}Fe_{0.85}Ti_{0.15}O_2$ phase increases. This phase represents a potassium ferrite phase with a limited of Ti that remains dissolved in it, suggesting that excess alkali promotes potassium ferrite production. Fan et al. [24] found that KFeO₂ was readily hydrolyzed during water leaching. However, minor Ti impurities in the KFeO₂ structure might inhibit the hydrolysis.

Figures 6d-f represent the XRPD patterns for the water leached residue of ilmenite samples roasted with different ratios of NaOH. The Na-Fe-Ti-O ternary phases and hematite are observed at the different stoichiometric amounts. These results partially agree with the phase equilibria calculations which predicted the formation of Fe₂O₃ and NaFeO₂, but not the presence of the ternary phase due to the lack of thermodynamic data available in the FACTSage database. Sodium ferrite undergoes the hydrolysis as described in equation (4) to form Fe₂O₃, which is in agreement with the E_h -pH diagram presented in figure 5b. Hematite precipitates as Fe(OH)₃ according to reaction (5), but heating of the residues converted this phase into Fe₂O₃ as observed in the XRPD patterns.

The XRPD patterns for the water-leached residues from KOH roasting show that only the K-Fe-Ti-O ternary phases were formed, whereas hematite, sodium titanate and the Na-Fe-Ti-O ternary phases are present in the NaOH patterns. This indicates that some of the alkali ferrite and alkali titanate were able to segregate from the Na-Fe-Ti-O ternary phase. The presence of the molten salt phase may inhibit this segregation and suggests that there may be less liquid present in the Na-Fe-Ti-O system than in the K-Fe-Ti-O system, as demonstrated by the phase diagrams in figure 4 and the phase equilibria calculations in table III. For both alkali salts the roasted samples fused to the crucible because of the formation of the liquid phase. In previous

studies organic acid leaching of roasted products containing ternary phases was carried in order to upgrade the TiO₂ content [11].

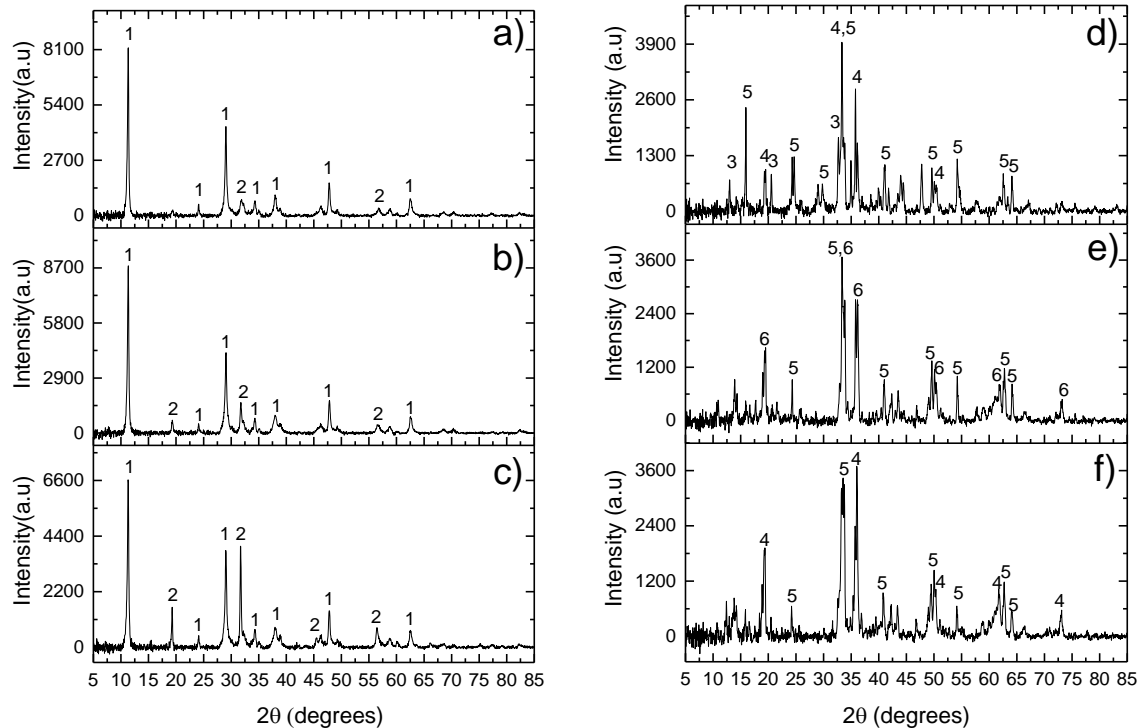


Figure 6. XRPD patterns of water leach residue after roasting ilmenite with a) stoichiometric KOH, b) 1.5 x stoichiometric KOH, c) 2 x stoichiometric KOH, d) stoichiometric NaOH, e) 1.5 x stoichiometric NaOH and f) 2 x stoichiometric NaOH. 1- $K_{0.4}Ti_{0.6}Fe_{0.4}O_2$ (04-010-9012), 2- $K_{0.85}Fe_{0.85}Ti_{0.15}O_2$ (00-062-0213), 3- $Na_2Ti_4O_9$ (04-011-2997), 4- $NaTiFeO_4$ (04-007-8937), 5- Fe_2O_3 (04-011-9586), 6- $Na_{2.65}Ti_{3.35}Fe_{0.65}O_9$ (04-014-6583)

Effect of roasting with KOH on ilmenite particle microstructure

Figure 7 is the backscattered SEM image of the water leach residue after roasting of ilmenite with 2 times the stoichiometric amount of KOH. Transgranular cracks can be observed throughout the microstructure of the particle. From the elemental mappings no significant segregation of the iron and titanium is observed, and this agrees with the XRPD results (figures 6a-c), where the two potassium iron titanates were the only products formed. Analysis of the edges of the transgranular cracks (Areas **A** and **C** in table IV) shows that the iron content at these points is higher than the titanium content, which indicates that the ilmenite particle is cracking along an iron-rich plane present within the lattice. Compositions of Areas **B** and **D** (in table IV) agree with the compositions expected from the dominant phase, $K_{0.4}Ti_{0.6}Fe_{0.4}O_2$, observed in the XRPD patterns (Figure 6c). Point **E** is an area with significantly more titanium than iron. Observing the SEM-EDX results presented in table IV, shows that there is limited variation in the composition throughout the particle.

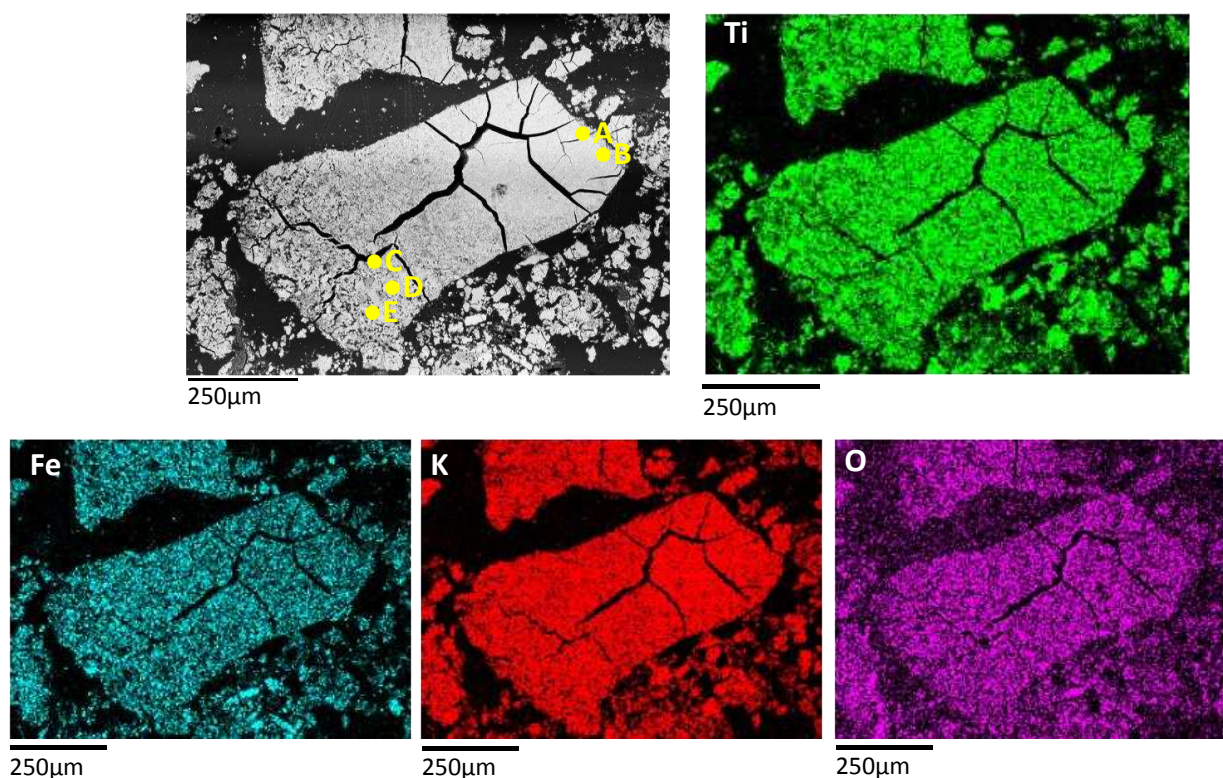


Figure 7. Backscattered SEM image and elemental mapping of water leached residue after roasting of ilmenite with 2 x stoichiometric ratio of KOH.

Table IV. Elemental composition of areas A to E in Figure 7 analysed by SEM-EDX.

%Wt	Ti	Fe	O	K	Mn	V
A	21.7	29.8	34.2	14.0	-	0.3
B	30.0	19.6	34.8	15.2	-	0.1
C	22.8	26.4	36.7	13.4	0.3	0.3
D	30.0	21.8	32.6	15.3	-	0.4
E	41.4	5.7	35.9	16.7	-	0.4

Effect of roasting with NaOH on ilmenite particle microstructure

The backscattered SEM of ilmenite roasted with 2 times the stoichiometric amount of NaOH and then water leached showed that there was segregation of an iron-rich phase and a titanium-rich phase, as illustrated by elemental mapping in figure 8. Table V clearly shows that the dark grey phase (Areas **A**, **C** and **E** in Table V) contain significant amounts titanium and a limited quantity of iron. Whereas the light grey phase (Area **D** in Table V) contains more iron with less titanium present. The SEM results agree with the XRPD patterns (figure 6d-f), which showed that some alkali ferrite was able to separate but also indicated the presence of Na-Fe-Ti-O ternary phases. Analysis of the transgranular crack edge (Area **B** on table V) shows that there is significantly more iron present than titanium, similarly to the sample roasted with KOH. This could be explained by the crack occurring along an iron-rich plane in the ilmenite lattice. Transgranular cracks within the microstructure of the particle are also observed in figure 8. However, these appear to be less extensive than when using KOH and this widespread

fracturing may have contributed to the fact that similar segregation of iron and titanium-rich phases was not seen in figure 7.

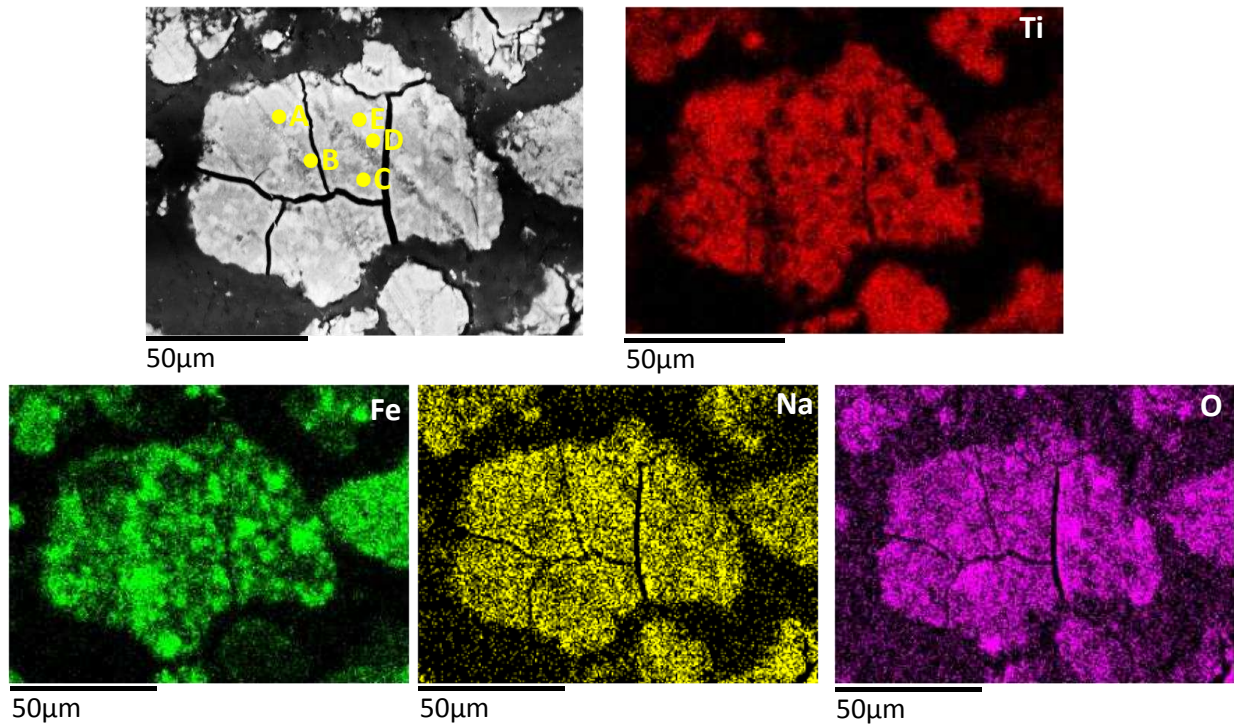


Figure 8. Backscattered SEM image and elemental mapping of water leached residue after roasting of ilmenite with 2 x stoichiometric ratio of NaOH.

Table V. Elemental composition of areas A to E in Figure 8 analysed by SEM-EDX.

%Wt	Ti	Fe	O	Na	Mn	V	Al
A	42.4	9.4	37.5	10.8	-	-	-
B	13.8	50.5	26.6	8.3	0.2	-	0.6
C	40.3	15.4	34.0	9.8	-	0.3	-
D	4.5	63.2	23.5	8.6	-	0.2	-
E	46.2	8.2	34.1	10.9	-	0.5	0.2

Ternary phases are produced by the partial substitution of Fe and/or Ti atoms in the ilmenite lattice by the alkali ions as they diffuse into the lattice during the roasting process [9]. Figures 9a and 9b illustrate ilmenite mineral crystals that have undergone partial substitution by potassium and sodium ions, respectively. The presence of alkali atoms leads to changes of the lattice along the c-axis [7]. The strain caused in the lattice structure results in cracking along the iron-rich planes, as observed in the analysis of the microstructure. Figures 7 and 8 demonstrated that the cracking was more extensive in the particles roasted with KOH than those roasted with NaOH, due to the larger atomic size of K⁺ ions (1.33 Å) compared to Na⁺ ions (0.97 Å) [8].

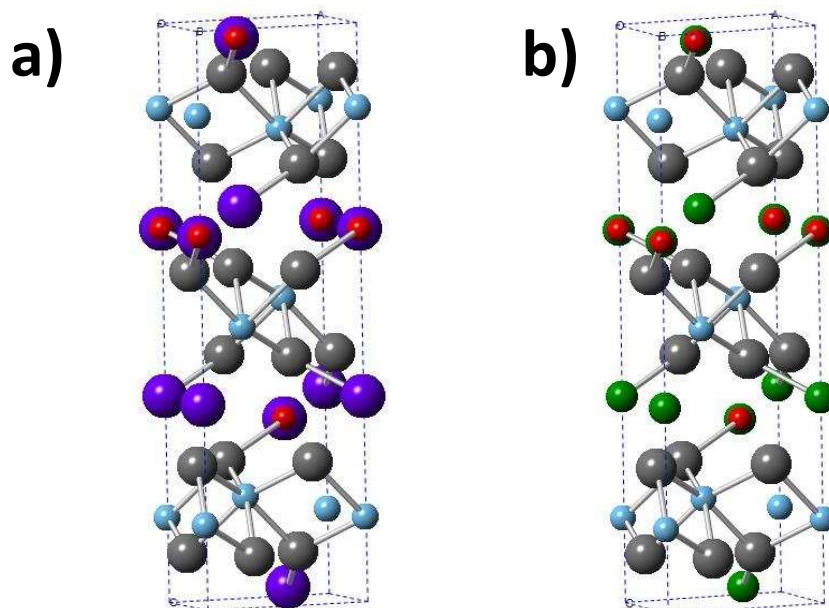


Figure 9. Crystal structure of ilmenite with partial atom substitution from roasting with a) KOH and b) NaOH. (O = grey, Ti = blue, Fe = red, K=purple, Na=green)

4. Conclusion

The phase diagrams for the M_2O - TiO_2 - Fe_2O_3 systems ($M=K$ or Na), calculated using FACTSage, showed that a liquid phase is expected for the roasting with KOH but not with NaOH. The equilibrium calculations performed for the various $FeTiO_3:MOH$ ratios (1:3, 1:4.5 and 1:6) demonstrated that sodium titanates were present at all stoichiometric ratios when utilising NaOH. However, in order to remove the iron in the ilmenite, two times the stoichiometric amount of NaOH is required to promote the formation of $NaFeO_2$.

Oxidative roasting of ilmenite with NaOH or KOH led to the formation of a molten phase as demonstrated by the fusion of the roasted sample to the alumina crucibles used. The XRPD patterns for the residues obtained from the water leaching of ilmenite roasted with NaOH showed that the phase equilibria calculations performed were partially accurate in predicting experimental results, since the phases present were Fe_2O_3 , sodium titanate and various sodium iron titanates. However, for the KOH roasting only K-Fe-Ti-O ternary phases were present. The microstructure analysis of the water leached residues after roasting with either KOH or NaOH showed that both alkali salts resulted in the formation of transgranular cracks, being the cracking process more extensive for the KOH case because of the larger size of K^+ ions. SEM-EDX analysis of the cracks edges shown a higher Fe content, indicating that the lattice fractures along the iron-rich planes. Segregation of iron and titanium was observed for the roasting with NaOH but this was not the case when using KOH, possibly due to the extensive fracturing occurred.

Acknowledgements

The authors acknowledge the financial support from the EPSRC standard grants ([GR/T08074/01](#) and [GR/L95977/01](#)) and PhD studentships for research which were initiated in 1997 at the University of Leeds. AJ also acknowledges the support from the European Union's Marie Curie Fellowship grant number [331385](#) for Dr. Sanchez-Segado and from the NERC's Catalyst Grant reference [NE/L002280/1](#). SP acknowledges the IoM³ for their support in the form of the Stanley Elmore Fellowship.

References

1. Kogel, J.E., *Industrial minerals & rocks: commodities, markets, and uses*. 2006: SME.
2. Auer, G., et al., *Pigments, Inorganic*, 2. White Pigments, in *Ullmann's Encyclopedia of Industrial Chemistry*. 2000, Wiley-VCH Verlag GmbH & Co. KGaA.
3. Cardarelli, F., *Materials Handbook: A Concise Desktop Reference*. 2008: Springer London.
4. Jha, A., The alkali roasting of complex oxide minerals for high purity chemicals-beyond the Le Chatelier era into the 21st century. *JOM*, 2011. **63**(1): p. 39-42.
5. Sanchez-Segado, S., et al., Reclamation of reactive metal oxides from complex minerals using alkali roasting and leaching—an improved approach to process engineering. *Green Chemistry*, 2015. **17**(4): p. 2059-2080.
6. Foley, E. and K.P. MacKinnon, Alkaline roasting of ilmenite. *Journal of Solid State Chemistry*, 1970. **1**(3-4): p. 566-575.
7. Lahiri, A. and A. Jha, Kinetics and Reaction Mechanism of Soda Ash Roasting of Ilmenite Ore for the Extraction of Titanium Dioxide. *Metallurgical and Materials Transactions B*, 2007. **38**(6): p. 939-948.
8. Lahiri, A. and A. Jha, Selective separation of rare earths and impurities from ilmenite ore by addition of K⁺ and Al³⁺ ions. *Hydrometallurgy*, 2009. **95**(3-4): p. 254-261.
9. Manhique, A.J., W.W. Focke, and C. Madivate, Titania recovery from low-grade titaniferous minerals. *Hydrometallurgy*, 2011. **109**(3-4): p. 230-236.
10. Sanchez-Segado, S., A. Lahiri, and A. Jha, Alkali roasting of bomar ilmenite: rare earths recovery and physico-chemical changes. *Open Chemistry*, 2015. **13**(1).
11. Parirenyatwa, S., et al., Comparative study of alkali roasting and leaching of chromite ores and titaniferous minerals. *Hydrometallurgy*, 2015.
12. Liu, X.-J., et al., Recovery of titanium and vanadium from titanium–vanadium slag obtained by direct reduction of titanomagnetite concentrates. *Rare Metals*, 2015: p. 1-9.
13. Tathavadkar, V. and A. Jha. The effect of molten sodium titanate and carbonate salt mixture on the alkali roasting of ilmenite and rutile minerals. in *VII International Conference on Molten Slags Fluxes and Salts*. 2004.
14. Wilson, N.C., et al., Structure and properties of ilmenite from first principles. *Physical Review B*, 2005. **71**(7): p. 075202.
15. Klein, C. and A. Philpotts, *Earth materials: introduction to mineralogy and petrology*. 2012: Cambridge University Press.
16. Teufer, G. and A.K. Temple, Pseudorutile—a New Mineral Intermediate between Ilmenite and Rutile in the N Alteration of Ilmenite. *Nature*, 1966. **211**(5045): p. 179-181.
17. Grey, I. and A. Reid, The structure of pseudorutile and its role in the natural alteration of ilmenite. *American Mineralogist*, 1975. **60**(9/10): p. 179-181.
18. Roine, A. and H. Outokumpu, *Chemistry for Windows: Chemical Reaction and Equilibrium Software with Extensive Thermodynamical Database, Version 5.1, User's Guide*. Outokumpu Research Oy, Finland, 2002.
19. Bale, C., et al., FactSage thermochemical software and databases. *Calphad*, 2002. **26**(2): p. 189-228.
20. Jha, A., et al., The Alkali Roasting and Leaching of Ilmenite Minerals for the Extraction of High Purity Synthetic Rutile and Rare-Earth Oxides, in *Energy Technology 2011*. 2011, John Wiley & Sons, Inc. p. 183-195.

21. Liu, Y., et al., Decomposition of ilmenite by concentrated KOH solution under atmospheric pressure. *International Journal of Mineral Processing*, 2006. **81**(2): p. 79-84.
22. Nayl, A.A. and H.F. Aly, Acid leaching of ilmenite decomposed by KOH. *Hydrometallurgy*, 2009. **97**(1-2): p. 86-93.
23. Nayl, A.A., N.S. Awwad, and H.F. Aly, Kinetics of acid leaching of ilmenite decomposed by KOH: Part 2. Leaching by H₂SO₄ and C₂H₂O₄. *Journal of Hazardous Materials*, 2009. **168**(2-3): p. 793-799.
24. Fan, L., et al., Potassium ferrites of KFeO₂ and K_{1+x}Fe₁₁O₁₇ systems (x = 0-1): Studies on leaching behavior in fused iron catalysts. *Journal of Solid State Chemistry*, 1990. **87**(2): p. 264-273.